Inorganic Chemistry

Article

pubs.acs.org/IC

New Yellow-Emitting Whitlockite-type Structure $Sr_{1.75}Ca_{1.25}(PO_4)_2:Eu^{2+}$ Phosphor for Near-UV Pumped White Light-Emitting Devices

Haipeng Ji,[†] Zhaohui Huang,*[,†] Zhiguo Xia,*[,†,‡] Maxim S. Molokeev,[§] Victor V. Atuchin,[∥,⊥,#] Minghao Fang,[†] and Saifang Huang[†]

[†]School of Materials Science and Technology, China University of Geosciences (Beijing), Beijing, 100083, China

[‡]School of Materials Sciences and Engineering, University of Science and Technology Beijing, Beijing 100083, China

[§]Laboratory of Crystal Physics, Kirensky Institute of Physics, SB RAS, Krasnoyarsk 660036, Russia

[∥]Laboratory of Optical Materials and Structures, Institute of Semiconductor Physics, SB RAS, Novosibirsk 630090, Russia

[⊥]Functional Electronics Laboratory, Tomsk State University, Tomsk 634050, Russia

[#]Laboratory of Semiconductor and Dielectric Materials, Novosibirsk State University, Novosibirsk 630090, Russia

Supporting Information

ABSTRACT: New compound discovery is of interest in the field of inorganic solid-state chemistry. In this work, a whitlockite-type structure $Sr_{1.75}Ca_{1.25}(PO_4)_2$ newly found by composition design in the $Sr_3(PO_4)_2$−$Ca_3(PO_4)_2$ join was reported. Crystal structure and luminescence properties of $Sr_{1.75}Ca_{1.25}(PO_4)_2:Eu^{2+}$ were investigated, and the yellow-emitting phosphor was further employed in fabricating near-ultraviolet-pumped white light-emitting diodes (w-LEDs). The structure and crystallographic site occupancy of Eu^{2+} in the host were identified via X-ray powder diffraction refinement using Rietveld method. The $Sr_{1.75}Ca_{1.25}(PO_4)_2:Eu^{2+}$ phosphors absorb in the UV−vis spectral region of 250−430 nm and exhibit an intense asymmetric broadband emission peaking at 518 nm under λ_{ex} = 365 nm which is ascribed to the 5d−4f allowed transition of Eu^{2+}. The luminescence properties and mechanism are also investigated as a function of Eu^{2+} concentration. A white LED device which is obtained by combining a 370 nm UV chip with commercial blue phosphor and the present yellow phosphor has been fabricated and exhibit good application properties.

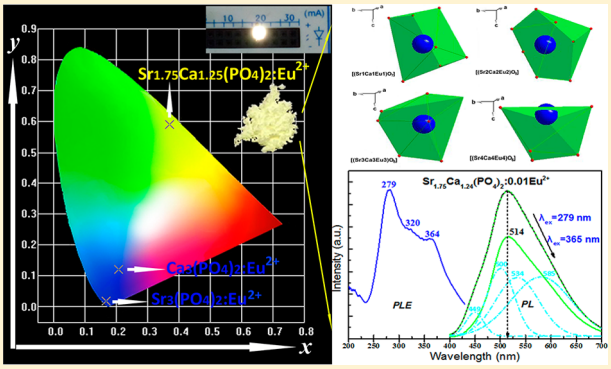

1. INTRODUCTION

White light emitting diodes (w-LEDs) are regarded as the next generation lighting source due to its outstanding merits of high energy efficiency, long lifetime, and environmental friendliness, in comparison to the conventional incandescent or fluorescence lamps.[1−4] In recent decades, solid-state lighting which relies on combination of phosphors and indium gallium nitride (InGaN) chip has attracted significant attention; red, green, and blue (RGB) phosphors play a key role in fabricating phosphor-converted (pc) w-LEDs devices.[5] Currently, the mostly used pc w-LEDs are produced by combining a blue LED chip with $Y_3Al_5O_{12}:Ce^{3+}$ (YAG:Ce) yellow phosphor. In addition to the famous YAG:Ce, the Eu^{2+}/Ce^{3+} doped yellow emitting phosphors have also been developed in the host systems including aluminates ($LaSr_2AlO_5:Ce^{3+}$),[6] silicates ($Sr_2SiO_4:Eu^{2+}$),[7] phosphates ($Ba_2Mg(PO_4)_2:Eu^{2+}$),[8] borates ($Ba_2Gd(BO_3)_2Cl:Eu^{2+}$),[9] and nitrides (Ca-α-SiAlON: Eu^{2+}).[10] The effort to develop suitable phosphor materials for application in w-LEDs is still ongoing.

Orthophosphate doped with rare earth ions is widely explored as RGB phosphors owing to advantages of relatively low sintering temperature, good chemical stability, and satisfactory absorption in the ultraviolent (UV)−near UV region. For example, the end members and some solid solution compositions in the $Sr_3(PO_4)_2$−$Ca_3(PO_4)_2$ join have been reported to be hosts for Eu^{2+}[11,12] and Eu^{3+}[13] activators. Both $Sr_3(PO_4)_2$ and $Ca_3(PO_4)_2$ are known to exhibit polymorphism on heating and cooling. Sarver et al.[14] reported the polymorphic nature of $Sr_3(PO_4)_2$: the α phase undergoes a rapid, reversible transition to the β modification at 1305 °C. The α phase crystallizes with monoclinic unit cell, and the β polymorph forms in a whitlockite-type structure of rhombohedral unit cell. As for $Ca_3(PO_4)_2$, β-$Ca_3(PO_4)_2$ is stable at room temperature (RT). α-$Ca_3(PO_4)_2$, stable between 1135 and 1430 °C, is quenchable to RT, whereas α'-$Ca_3(PO_4)_2$, stable

Received: January 29, 2014
Published: April 29, 2014

   dx.doi.org/10.1021/ic500230v | Inorg. Chem. 2014, 53, 5129−5135

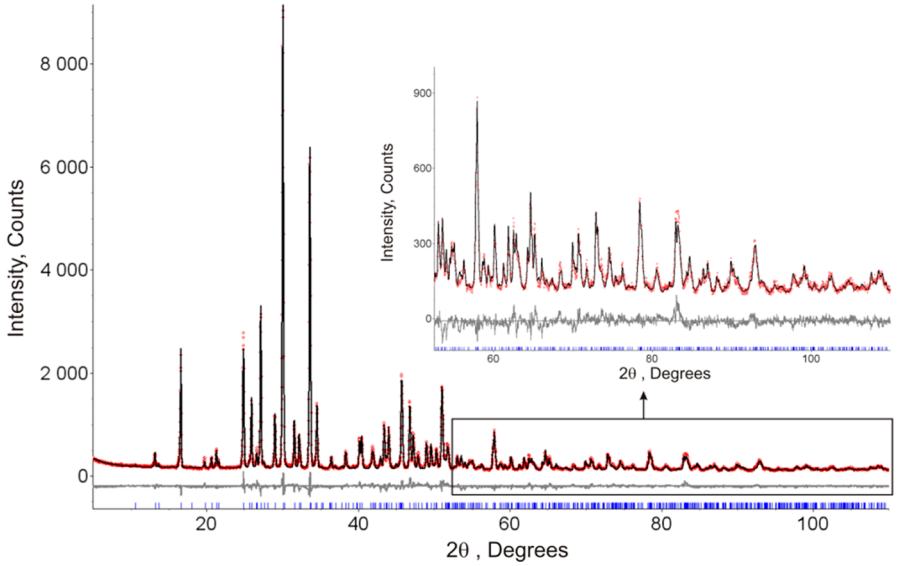

Figure 1. Observed (red), calculated (black), and difference (gray) synchrotron XRD profiles for the refinement of the sample $Sr_{1.75}Ca_{1.15}Eu_{0.1}(PO_4)_2$ by Rietveld method. Bragg reflections are indicated with tick marks.

above 1430 °C, is not quenchable.[15] The polymorphic transition that resulted from sintering temperature or cation impurity stabilizing phenomenon may induce tunable color emission of Eu^{2+} in the solid solution phases.

In our attempt to explore the luminescence of Eu^{2+} in compositions of the $Sr_3(PO_4)_2$−$Ca_3(PO_4)_2$ join, it is interestingly observed that, under an identical sintering procedure (holding temperature at 1250 °C and cooling rate of ∼10 °C/min), the end members $Sr_3(PO_4)_2$ (α type with space group of $R\bar{3}m$) and $Ca_3(PO_4)_2$ (β type with space group of $R3c$) doped with Eu^{2+} ions emit bluish-purple light peaking at 416 nm, whereas the selected compositions with a proper amount of Ca^{2+} substituting Sr^{2+} show yellow light emitting; the corresponding emission peak even gets red-shifted to be 534 nm. The distinctive luminescence evolution of Eu^{2+} suggests the formation of a new phase that may have a similar space group with either of the end members but with different cell parameters. New compound discovery is of great interest to a board range of research fields including materials, crystal physics, and chemistry.[16,17] Particularly, among the $Sr_{3-x}Ca_x(PO_4)_2$ string compositions with interval x of 0.25, the $Sr_{1.75}Ca_{1.25}(PO_4)_2$:$Eu^{2+}$ attracts much our attention because of its yellow-emitting merit and relatively excellent luminescence property.

The aim of this study is the observation of spectroscopic properties of $Sr_{1.75}Ca_{1.25}(PO_4)_2$:$Eu^{2+}$ in relation with its crystal structure information and practical application in w-LEDs. The X-ray diffraction (XRD) pattern of $Sr_{1.75}Ca_{1.25}(PO_4)_2$ phase is preliminarily found to be similar to the whitlockite mineral which crystallizes in the space group $R3c$.[18] In a typical whitlockite structure compound like β-$Ca_3(PO_4)_2$, there exist five different kinds of cationic crystallographic sites.[19] The occupancy of Eu^{2+} in these sites is of diversity, resulting in interesting crystal chemistry and adjustable crystal field environment. The doping cation sites and the crystal field environment around activators are demonstrated to play a crucial role influencing the luminescence properties.[20−22] In the $Sr_{1.75}Ca_{1.25}(PO_4)_2$ host, it is difficult to predict whether Eu^{2+} ions randomly occupy the cation sites or prefer to enter some specific sites. In addition to the exploration of the photoluminescence property, this work is also aimed to investigate the structural property of $Sr_{1.75}Ca_{1.25}(PO_4)_2$:$Eu^{2+}$ by XRD refinement. Furthermore, a near-UV w-LED lamp using the yellow emitting $Sr_{1.75}Ca_{1.25}(PO_4)_2$:$Eu^{2+}$ and commercial blue-emitting $BaMgAl_{10}O_{17}$:Eu^{2+} (BAM:Eu) in combination with a 370 nm UV LED chip is successfully fabricated, and the optical properties of the device are examined. The results indicate that the reported phosphor can serve as a yellow component for application in the near-UV w-LEDs.

2. EXPERIMENTAL SECTION

2.1. Materials and Synthesis. The $Sr_{1.75}Ca_{(1.25-x)}(PO_4)_2$:$xEu^{2+}$ (x = 0−0.15) powder samples were synthesized by the high temperature solid-state reaction method. The starting materials, $SrCO_3$ (A.R. grade), $CaCO_3$ (A.R. grade), $NH_4H_2PO_4$ (A.R. grade), and Eu_2O_3 (99.99% purity), were stoichiometrically weighed and thoroughly mixed by an agate mortar and pestle. First, the mixtures were preheated at 700 °C for 2 h in a muff furnace in air to release NH_3, CO_2, and H_2O. Then, the precursor was reground and heated at 1250 °C for 5 h in a tube furnace under flowing 5% H_2−95% N_2 reducing atmosphere. Finally, the samples were furnace-cooled to room temperature with cooling rate of ∼10 °C/min. A near-UV w-LED lamp was fabricated using a mixture of silicon resin and phosphor blend of the as-prepared yellow-emitting $Sr_{1.75}Ca_{1.25}(PO_4)_2$:$Eu^{2+}$ and commercial blue-emitting $BaMgAl_{10}O_{17}$:Eu^{2+}, which were dropped onto a 370 nm UV chip.

2.2. Characterization. The elemental composition of the phosphor was quantitatively analyzed by the inductively coupled plasma atomic emission spectroscopy (ICP-OES; IRIS Intrepid II XSP, Thermo Scientific). The powder diffraction pattern of $Sr_{1.75}Ca_{1.15}Eu_{0.10}(PO_4)_2$ for Rietveld analysis was collected at room temperature with a Bruker D8-ADVANCE powder diffractometer (Cu Kα radiation) and a linear VANTEC detector. The step size of 2θ was 0.016°, and the counting time was 1 s per step. Rietveld refinement was performed by using TOPAS 4.2.[23] Room temperature excitation and emission spectra were measured on a fluorescence spectrophotometer (F-4600, HITACHI, Japan) with a photomultiplier tube operating at 400 V, and a 150 W Xe lamp used as the excitation source. The morphology was observed using scanning electron microscopy (SEM; JSM-6460LV, JEOL, Japan) and high-resolution transmission electron microscopy (HRTEM; JEM-2010, JEOL, Japan). The energy dispersive X-ray spectroscopy (EDS, INCA, Oxford instruments, U.K.) linked with the HRTEM was used to assist the composition

dx.doi.org/10.1021/ic500230v | Inorg. Chem. 2014, 53, 5129−5135

determination. The diffuse reflection spectra were measured using a UV−vis−NIR spectrophotometer (SHIMADZU UV-3600) attached with an integrating sphere. $BaSO_4$ was used as a reference for 100% reflectance. The optical properties, including the luminescent spectrum, R_a, CCT, and CIE value of the fabricated w-LED lamp, were measured by a HAAS-2000 light and radiation measuring instrument (Everfine, China).

3. RESULTS AND DISCUSSION

3.1. Crystal Structure Refinement and Micromorphology of $Sr_{1.75}Ca_{1.25}(PO_4)_2:Eu^{2+}$. Under the present sintering process, the end members $Sr_3(PO_4)_2$ and $Ca_3(PO_4)_2$ are found to crystallize in space groups $R\bar{3}m$ and $R3c$, respectively. Thus, it is expected that the samples with composition falling between the two end members would prefer to form partial solid solutions rather than complete solid solution, indicating that pure-phase confirmation of $Sr_{1.75}Ca_{1.25}(PO_4)_2$ is really necessary. However, no Inorganic Crystal Structure Database (ICSD) or Joint Committee on Powder Diffraction Standards (JCPDS) file for the $Sr_{1.75}Ca_{1.25}(PO_4)_2$ is available. The selected sample $Sr_{1.75}Ca_{1.15}Eu_{0.1}(PO_4)_2$ is then refined using the Rietveld method. The single crystal structure data of $Ca_{2.83}Sr_{0.17}(PO_4)_2$ (ICSD No. 161330; whitlockite-type structure)[24] is used as a starting model to refine the crystal structure. The observed (red), calculated (black), and difference (gray) XRD profiles for the refinement are shown in Figure 1. There are five independent Ca positions in the structure. In our model all of these positions were occupied by Ca and Sr, and occupation was refined; after refinement the Ca5/Sr5 position has Ca ion occupation equaling 1.00(1) and Sr ion occupation 0.0(1). Analysis of Ca5/Sr5−O bond lengths shows that this site is very small for Sr and Eu ions; therefore, it was decided to occupy this position by Ca ion only. The other four sites can be occupied by Sr and Eu ions. Eu ions were equally distributed between the four Ca/Sr positions, and their concentrations were fixed in these sites. The structure refinement was stable and ended with low R-factors (shown in Table 1, Figure 1).

Table 1. Crystallographic Data and Details in the Data Collection and Refinement Parameters for the $Sr_{1.75}Ca_{1.15}Eu_{0.10}(PO_4)_2$ Sample

	$Sr_{1.75}Ca_{1.15}Eu_{0.1}(PO_4)_2$
space group	$R3c$
a, Å	10.6498(3)
c, Å	38.787(1)
V, Å^3	3809.8(2)
Z	21
2θ-interval, deg	5−110
no. reflns	546
no. params of refinement	84
R_{wp}, %	8.30
R_p, %	6.26
R_{exp}, %	6.22
χ^2	1.33
R_B, %	3.47

When doped with 0.10 mol Eu^{2+} per mol Ca^{2+} ions, the $Sr_{1.75}Ca_{1.25}(PO_4)_2$ host persists the single-phase structure. The refinement shows that $Sr_{1.75}Ca_{1.15}Eu_{0.1}(PO_4)_2$ crystallizes in a rhombohedral unit cell with space group $R3c$ and lattice constants of a = 10.6498(3) Å and c = 38.787(1) Å, and cell volume V = 3809.8(2) Å^3. The refinement is finally converged to R_{exp} = 6.22, R_{wp} = 8.30, and R_p = 6.26 (Table 1). The crystal structure is shown in Figure 2. Figure 2 also presents that the Sr1/Ca1, Sr2/Ca2, Sr3/Ca3, and Sr4/Ca4 positions are

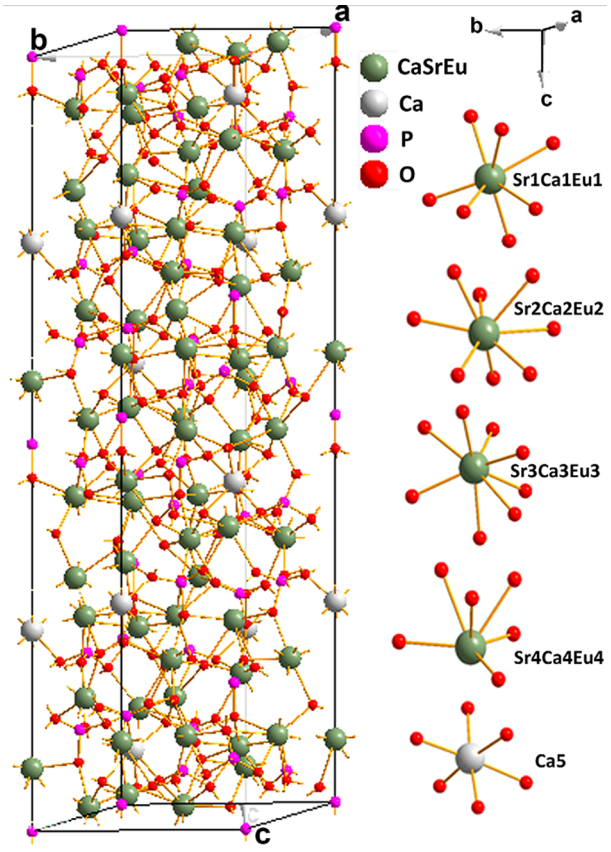

Figure 2. (a) Crystal structure of the sample $Sr_{1.75}Ca_{1.15}Eu_{0.10}(PO_4)_2$, and (b) coordination of the cation ions with oxygen atoms.

coordinated with seven, eight, eight, and six oxygen atoms, and the Ca5 position is coordinated with six oxygen atoms. Crystallographic information file (CIF) of $Sr_{1.75}Ca_{1.15}Eu_{0.1}(PO_4)_2$ is given in Supporting Information.

The elemental composition of sample with nominal formula $Sr_{1.75}Ca_{1.15}$ $Eu_{0.10}(PO_4)_2$ verified by ICP-AES shows (wt %) Sr 38.05%, Ca 11.43%, Eu 3.690%, and P 15.60%. The stoichiometric weight ratio of each element in $Sr_{1.75}Ca_{1.15}Eu_{0.10}(PO_4)_2$ is Sr 37.772%, Ca 11.354%, Eu 3.743%, and P 15.26%. The composition suggested by ICP-AES is consistent with the stoichiometric weight ratio with reasonable relative error. Coexistence and the element distribution of Sr, Ca, P, O, and Eu in the solid-solution sample was also verified by the HRTEM and corresponding EDS analysis, as shown in Figure 3. Figure 3a shows the TEM image obtained from the selected $Sr_{1.75}Ca_{1.15}Eu_{0.10}(PO_4)_2$ crystal, and all the elements (including the C and Cu from the sample holder) were detected from one complete microcrystal (Figure 3d). The fine structures are further examined by HRTEM, and the fast Fourier transform (FFT) images suggest the highly single-crystalline nature, as shown in Figure 3b,c. It could be seen that the continuous lattice fringe measurements with d spacing of 0.308 and 0.283 nm are in line with the solved structure of the compound by refinement, and could be assigned to the corresponding (030) and (042) planes, respectively.

dx.doi.org/10.1021/ic500230v | Inorg. Chem. 2014, 53, 5129−5135

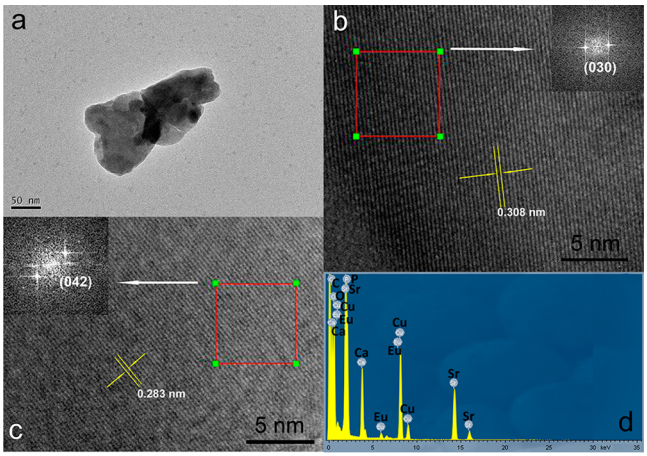

Figure 3. (a) TEM image, (b and c) HRTEM images of $Sr_{1.75}Ca_{1.15}Eu_{0.10}(PO_4)_2$ and (d) EDS pattern detected in (a). Inserts in parts b and c are the fast Fourier transforms (FFTs) of the relevant HRTEM images.

The micromorphology of the crystalline $Sr_{1.75}Ca_{1.24}(PO_4)_2$:0.01$Eu^{2+}$ phosphor sample observed by SEM is shown in Figure 4. It is observed that the particles have

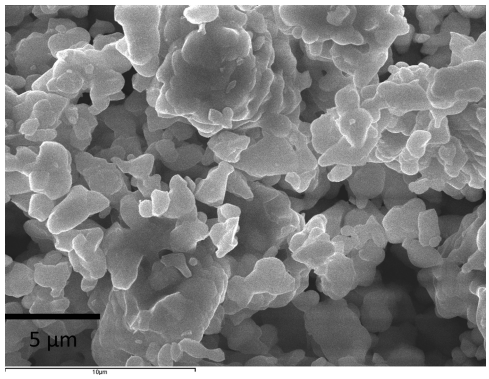

Figure 4. SEM image of the as-prepared $Sr_{1.75}Ca_{1.25}(PO_4)_2$:$Eu^{2+}$ phosphor.

smooth morphology and the diameters are ranging from 3 to 8 μm. Some of the primary crystals reunited to yield agglomerates, and the observed "sintering necks" are suggesting that grain growth has occurred during the synthesis procedure. Without further hard crush, the as-prepared microphosphor particles can be used for w-LED fabrication.

3.2. Photoluminescence Properties of $Sr_{1.75}Ca_{1.25}(PO_4)_2$:$Eu^{2+}$. Figure 5 illustrates the photoluminescence excitation and emission spectra of $Sr_{1.75}Ca_{1.24}(PO_4)_2$:0.01$Eu^{2+}$. The broad asymmetric emission spectrum peaking at 514 nm shows that Eu^{2+} has more than one emission center in $Sr_{1.75}Ca_{1.25}(PO_4)_2$ which belongs to the typical emission of Eu^{2+} ions ascribed to 5d−4f transitions.[25] The excitation spectrum monitoring at 514 nm is composed of three absorption peaks located at 279, 320, and 364 nm in the spectral range from 200 to 430 nm. Since phosphate hosts exhibit absorption in the vacuum ultraviolet region (100−200 nm),[26] the excitation band in the range of 230−430 nm is originated from the $4f^7(^8S_{7/2})$ ground state to 4f $^65d^1$ excited state transition of Eu^{2+} ions. Under the excitation at 279 and 365 nm, the phosphor exhibited similar broad yellow emission band peaking at 514 nm. No dependence of the emission spectra on the excitation

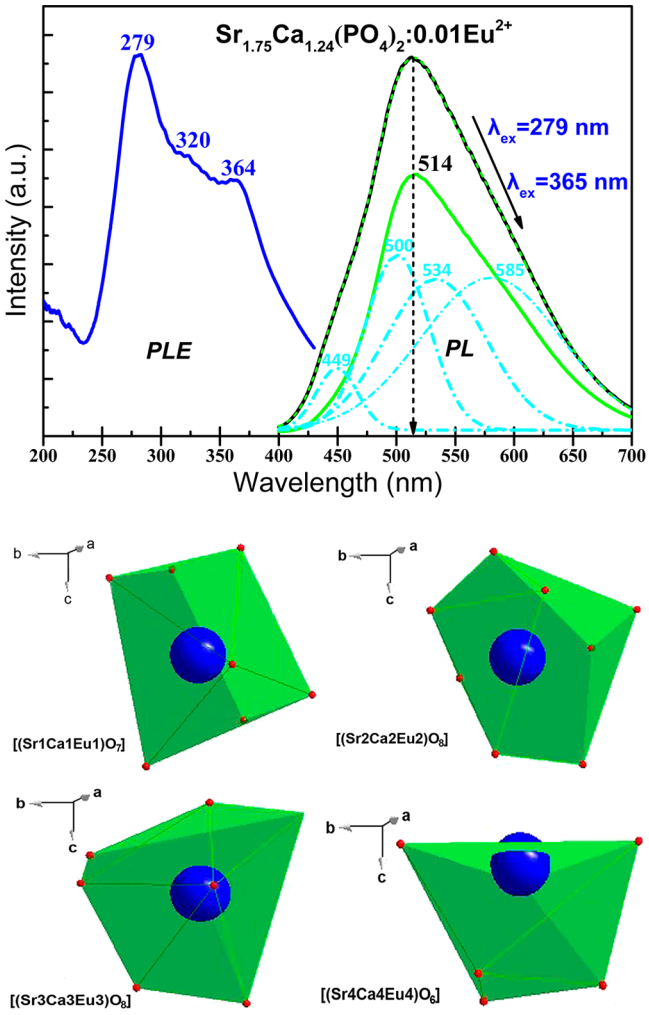

Figure 5. Excitation (λ_{em} = 514 nm) and emission (λ_{ex} = 279 and 365 nm) spectra of $Sr_{1.75}Ca_{1.24}(PO_4)_2$:0.01$Eu^{2+}$. Four kinds of polyhedra are illustrated to correspond to four Gaussian emission peaks.

wavelengths was found. The broadband excitation character in 200 and 430 nm of the excitation spectrum verifies the possibility of the operation as a yellow-emitting phosphor combining with the near-UV LEDs chip (λ_{em}: 350−410 nm), especially the excitation wavelength at 365 nm that can be found from typical commercial chips.

By Gaussian deconvolution, the emission spectrum of $Sr_{1.75}Ca_{1.24}(PO_4)_2$:0.01$Eu^{2+}$ can be well-decomposed into four Gaussian profiles peaking at 449 nm (22 271 cm^{-1}), 500 nm (20 000 cm^{-1}), 534 nm (18 726 cm^{-1}), and 589 nm (16 978 cm^{-1}) which can be ascribed to four different Ca^{2+} sites occupied by Eu^{2+} ions. The refinement shows that the structure of $Sr_{1.75}Ca_{1.25}(PO_4)_2$ contains four crystallographically distinct Ca^{2+} sites that can be occupied by Eu^{2+} with average Ca−O band distance as follows: Ca(1)−O 2.621 Å, Ca(2)−O 2.555 Å, Ca(3)−O 2.604 Å, and Ca(4)−O 2.655 Å. The Eu^{2+} ions substituting Ca^{2+} ions in the site which has shorter Ca−O band distance are expected to experience stronger crystal field strength corresponding to a longer wavelength emission with larger Stoke shift, when the crystal environments are analogous. Figure 5 illustrates four kinds of polyhedra with different average Ca−O band distance, corresponding to the four Gaussian profiles in the emission spectrum. Moreover, due to the straightforward symmetry behavior of the energy levels,

dx.doi.org/10.1021/ic500230v | Inorg. Chem. 2014, 53, 5129−5135

$Sr_{1.75}Ca_{1.25}(PO_4)_2$ doped with Eu^{3+} was prepared following the identical sintering procedure in air, to use Eu^{3+} as a probe to determine the local structure symmetry. The PL spectrum of $Sr_{1.75}Ca_{1.25}(PO_4)_2$:$Eu^{3+}$ (Supporting Information Figure S1) shows strong emission at 616 nm along with a relatively weak emission at 592 nm, suggesting that the symmetry around the Eu^{3+} ions in the host is low, a fact confirming the crystallographic sites occupancy of Eu^{2+} in $Sr_{1.75}Ca_{1.25}(PO_4)_2$ identified by the refinement.

Figure 6 exhibits the UV−vis reflection spectra of undoped and Eu^{2+}-doped $Sr_{1.75}Ca_{1.25}(PO_4)_2$ samples. The $Sr_{1.75}Ca_{1.25}$-

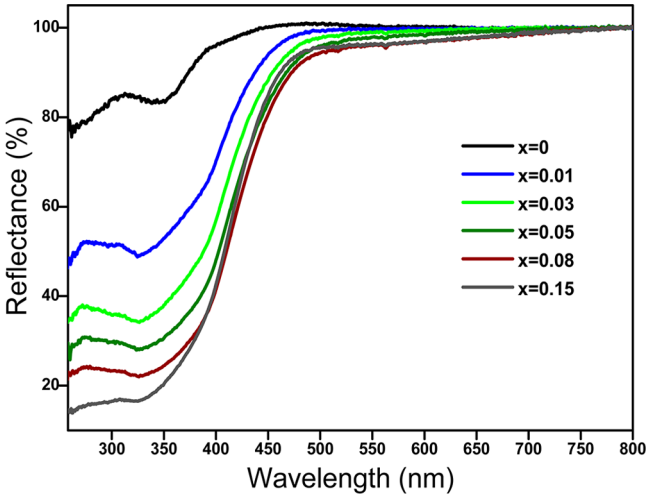

Figure 6. Diffuse reflectance spectra of $Sr_{1.75}Ca_{(1.25-x)}(PO_4)_2$:$xEu2^+$ (x = 0−0.15) samples.

$(PO_4)_2$ host demonstrates an absorption edge in the ≤420 nm region. With the introduction of Eu^{2+} ions in $Sr_{1.75}Ca_{1.25}(PO_4)_2$, a broad absorption appears in the range 300−460 nm which originated from the $4f^7$−$4f^65d^1$ transition of Eu^{2+}, which matches well with near-UV chips for applications in near-UV w-LEDs. Also, the absorption edge gradually extends to longer wavelengths, and the absorption gets enhanced with higher Eu^{2+} concentration.

Figure 7 presents the room temperature emission spectra of $Sr_{1.75}Ca_{(1.25-x)}(PO_4)_2$:$xEu^{2+}$ (x = 0.005−0.150) under 365 nm UV light excitation. With an increasing Eu^{2+} doping level, the emission intensity of $Sr_{1.75}Ca_{(1.25-x)}(PO_4)_2$:$xEu^{2+}$ initially increased, reached the maximum at x = 0.01, and then decreased, resulting from the concentration quenching effect. The inset of Figure 7a shows the dependence of the emission intensity on the concentration of Eu^{2+}, suggesting the optimum doping amount of Eu^{2+} to be x = 0.01. It is also observed that the emission peak of the samples has shifted to the longer wavelength region (from 515 to 523 nm) (Figure 7b) with increasing concentration of Eu^{2+}. As assumed from related reports, due to the increase in doping concentration of Eu^{2+}, the interatomic distance between two activators is expected to become shorter, and the interaction is enhanced.[27] The crystal field strength surrounding Eu^{2+} is thus increased, resulting in the red-shifting of the emission peak. Previous literature[28,29] also confirms the red shift of the emission peak in rare earth doped phosphors with increasing doping concentration due to the variations of crystal field strength surrounding the activators. Here, in addition to the red shift of the emission peak, the intensity of the ∼450 nm emission gets inhibited

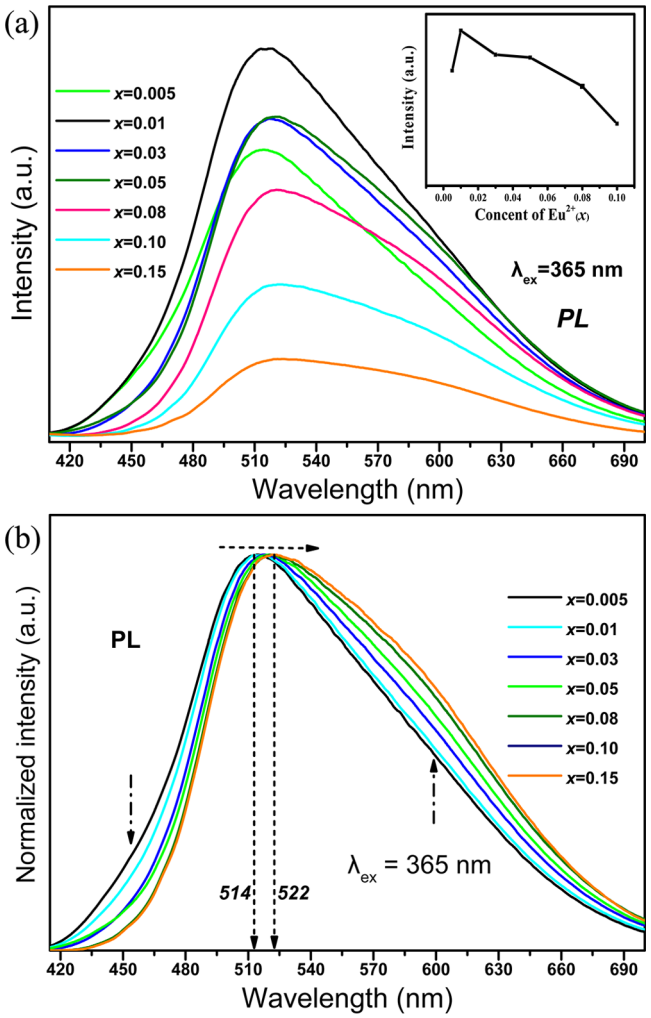

Figure 7. (a) Emission spectra of $Sr_{1.75}Ca_{(1.25-x)}(PO_4)_2$:$xEu^{2+}$ (x = 0.005−0.15) phosphors under 365 nm UV light excitation. The inset shows the dependence of the emission intensity on the concentration of Eu^{2+}. (b) Normalized emission spectra of $Sr_{1.75}Ca_{(1.25-x)}$-$(PO_4)_2$:xEu^{2+} (x = 0.005−0.15) phosphors under 365 nm UV light excitation.

while that of the ∼600 nm emission gets enhanced with increasing concentration of Eu^{2+} (Figure 7b). Although the intrinsic explanation is still unknown, it suggests that Eu^{2+} prefers to occupy some specific sites at high doping level. It is known that the interaction type between sensitizers or between sensitizer and activator can be calculated by the following eq 1:[30]

$$I/x = k[1 + \beta(x)^{\theta/3}]^{-1} \quad (1)$$

Here, x is the activator concentration, I/x is the emission intensity (I) per activator concentration (x), k and β are constants for the same excitation condition, and θ is a function of multipole−multipole interaction. When the value of θ is 6, 8, or 10, the form of the interaction corresponds to dipole−dipole (d−d), dipole−quadrupole (d−q), or quadrupole−quadrupole (q−q), respectively.[31] To get the θ value, the relationship between lg (I/x) and lg (x) is plotted in Figure 8. The slope of the straight line is −1.3691 which equals $-\theta/3$. Thus, the value of θ is calculated to be 4.1073, which is mostly close to 6, suggesting that the quenching in $Sr_{1.75}Ca_{1.25}(PO_4)_2$:$Eu^{2+}$ phosphors most likely results from dipole−dipole interactions.

dx.doi.org/10.1021/ic500230v | Inorg. Chem. 2014, 53, 5129−5135

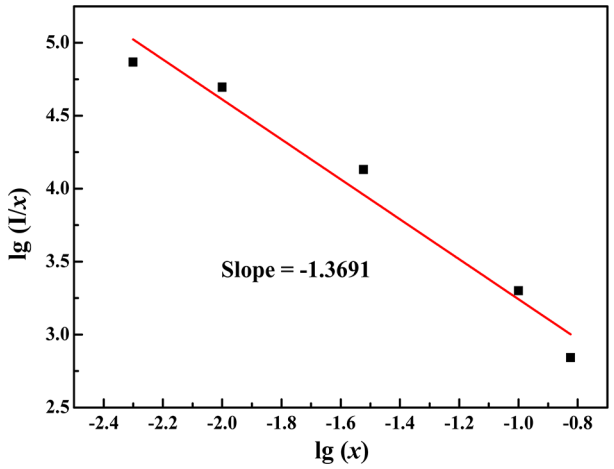

Figure 8. Relationship between the lg(I/x) and lg(x) of $Sr_{1.75}Ca_{1.25}(PO_4)_2$:$Eu^{2+}$ phosphors.

3.3. Performances of the Fabricated Near-UV w-LEDs.

The CIE chromaticity diagram for $Sr_{1.75}Ca_{1.24}(PO_4)_2$:$0.01Eu^{2+}$ under 365 nm light excitation is shown in Figure 9a. The color coordinates are calculated to be (x = 0.374, y = 0.588), indicating this phosphor may serve as a yellow emitting component for w-LED application. The inset in Figure 9a shows the digital photograph of $Sr_{1.75}Ca_{1.24}(PO_4)_2$:$0.01Eu^{2+}$, the intense yellow emission of which can be observed. To evaluate the potential application of $Sr_{1.75}Ca_{1.25}(PO_4)_2$:$Eu^{2+}$ in w-LED, we combined mixtures of this phosphor and commercial blue-emitting $BaMgAl_{10}O_{17}$:Eu^{2+} (BAM:Eu) with 370 nm UV chip to realize white light. Figure 9b shows the electroluminescent (EL) spectrum of the fabricated w-LED prototype. The blue emission band is ascribed to BAM:Eu, and the yellow emission band corresponds to $Sr_{1.75}Ca_{1.25}(PO_4)_2$:$Eu^{2+}$; the full-color white light emission is achieved. The color coordinate is calculated to be (0.368, 0.414) with the white light emission correlated color temperature (CCT) of 4529 K and good CRI value (R_a) determined as 85.1.

4. CONCLUSIONS

On the basis of the composition design in the $Sr_3(PO_4)_2$–$Ca_3(PO_4)_2$ join, a new yellow-emitting whitlockite-type structure phosphor $Sr_{1.75}Ca_{1.25}(PO_4)_2$:$Eu^{2+}$ has been discovered, and its crystal structure is refined to be rhombohedral unit cell with space group $R3c$ and lattice constants a = 10.6498(3) Å and c = 38.787(1) Å, and cell volume = 3809.8(2) $Å^3$ using the Rietveld method. It exhibits a broad emission band peaking at 514 nm which is ascribed to the 5d–4f transition of Eu^{2+}. The dipole–dipole interaction plays a major role in the explanation of the concentration quenching effect. The w-LED is encapsulated with a 370 nm-emitting chip, and the as-prepared $Sr_{1.75}Ca_{1.25}(PO_4)_2$:$Eu^{2+}$ and commercial blue-emitting $BaMgAl_{10}O_{17}$:Eu^{2+} exhibit bright white emission, indicating that $Sr_{1.75}Ca_{1.25}(PO_4)_2$:$Eu^{2+}$ can serve as a potential yellow component candidate for near-UV w-LED fabrication.

■ ASSOCIATED CONTENT

Supporting Information

CIF file of $Sr_{1.75}Ca_{1.15}Eu_{0.10}(PO_4)_2$ and photoluminescence spectrum of $Sr_{1.75}Ca_{1.25}(PO_4)_2$:$Eu^{3+}$. This material is available free of charge via the Internet at http://pubs.acs.org.

■ AUTHOR INFORMATION

Corresponding Authors

*E-mail: huang118@cugb.edu.cn (Z.H.).
*E-mail: xiazg@ustb.edu.cn (Z.X.).

Notes

The authors declare no competing financial interest.

■ ACKNOWLEDGMENTS

This work was supported by the National Natural Science Foundations of China (Grant Nos. 51032007, 51002146, 51272242), the Research Fund for the Doctoral Program of Higher Education of China (Grant No. 20130022110006), and the Program for New Century Excellent Talents in University of Ministry of Education of China (NCET-12-0950). V.V.A. gratefully acknowledges the Ministry of Education and Science of the Russian Federation for the financial support. S.H. would like to acknowledge the China Scholarship Council (CSC) for

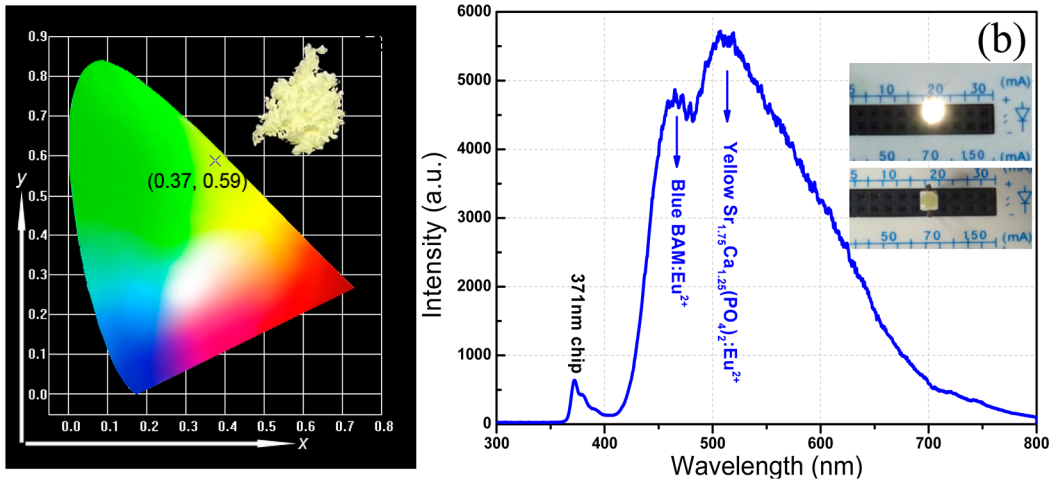

Figure 9. (a) Color coordinate of $Sr_{1.75}Ca_{1.24}(PO_4)_2$:$0.01Eu^{2+}$ under λ_{ex} = 365 nm in the CIE chromaticity diagram (a digital image of the phosphor under 365 nm UV lamp revealing an intense yellow light is shown in the inset). (b) Electroluminescent spectrum of a white LED prototype encapsulated with a 370 nm UV chip and as-prepared $Sr_{1.75}Ca_{1.25}(PO_4)_2$:$Eu^{2+}$ and commercial $BaMgAl_{10}O_{17}$ (BAM):Eu^{2+} blue emitting phosphor (digital images of the lamp with and without powder input are shown in the inset).

dx.doi.org/10.1021/ic500230v | Inorg. Chem. 2014, 53, 5129–5135

providing a doctoral scholarship for his Ph.D. study at the University of Auckland.

REFERENCES

(1) Nakamura, S.; Fasol, G. *The Blue Laser Diode, GaN Based Light Emitters and Lasers*; Springer: Berlin, Germany, 1997.
(2) Schnick, W. *Phys. Status Solidi RRL* **2011**, *3*, A113−4.
(3) Xie, R. J.; Hirosaki, N. *Sci. Technol. Adv. Mater.* **2007**, *8*, 588−600.
(4) Lin, C. C.; Liu, R. S. *J. Phys. Chem. Lett.* **2011**, *2*, 1268−77.
(5) Höppe, H. A. *Angew. Chem., Int. Ed.* **2009**, *48*, 3572−82.
(6) Im, W. B.; Fellows, N. N.; DenBaars, S. P.; Seshadri, R.; Kim, Y. I. *Chem. Mater.* **2009**, *21*, 2957−66.
(7) Yoo, J. S.; Kim, S. H.; Yoo, W. T.; Hong, G. Y.; Kim, K. P.; Rowland, J.; Holloway, P. H. *J. Electrochem. Soc.* **2005**, *152*, G382−5.
(8) Wu, Z. C.; Gong, M. L.; Shi, J. X.; Wang, G.; Su, Q. A. *Chem. Lett.* **2007**, *36*, 410−1.
(9) Xia, Z. G.; Zhang, J. Q.; Liao, L. B.; Liu, H. K.; Luo, Y.; Du, P. *J. Electrochem. Soc.* **2011**, *158*, J359−62.
(10) Xie, R. J.; Hirosaki, N.; Sakuma, K.; Yamamoto, Y.; Mitomo, M. *Appl. Phys. Lett.* **2004**, *84*, 5404−6.
(11) Lagos, C. C. *J. Electrochem. Soc.* **1970**, *117*, 1189−93.
(12) Poort, S. H. M.; Van Krevel, J. W. H.; Stomphorst, R.; Vink, A. P.; Blasse, G. *J. Solid State Chem.* **1996**, *122*, 432−5.
(13) Zhang, X. G.; Zhou, L. Y.; Gong, M. L. *Opt. Mater.* **2013**, *35*, 993−7.
(14) Sarver, J. F.; Hoffman, M. V.; Hummel, F. A. *J. Electrochem. Soc.* **1961**, *108*, 1103−10.
(15) Belik, A. A.; Izumi, F.; Stefanovich, S. Yu.; Malakho, A. P.; Lazoryak, B. I.; Leonidov, I. A.; Leonidova, O. N.; Davydov, S. A. *Chem. Mater.* **2002**, *14*, 3197−205.
(16) Park, W. B.; Son, K. H.; Singh, S. P.; Sohn, K. S. *ACS Comb. Sci.* **2012**, *14*, 537−44.
(17) Park, W. B.; Singh, S. P.; Sohn, K. S. *J. Am. Chem. Soc.* **2014**, *136*, 2363−73.
(18) Lazoryak, B. I.; Strunenkova, T. V.; Golubev, V. N.; Vovk, E. A.; Ivanov, L. N. *Mater. Res. Bull.* **1996**, *31*, 207−16.
(19) Yashima, M.; Sakai, A.; Kamiyama, T.; Hoshikawa, A. *J. Solid State Chem.* **2003**, *175*, 272−7.
(20) Im, W. B.; Kim, Y. I.; Yoo, H. S.; Jeon, D. Y. *Inorg. Chem.* **2008**, *48*, 557−64.
(21) Xia, Z. G.; Wang, X. M.; Wang, Y. X.; Liao, L. B.; Jing, X. P. *Inorg. Chem.* **2011**, *50*, 10134−42.
(22) Lv, W.; Jia, Y. C.; Zhao, Q.; Lv, W. Z.; You, H. P. *Chem. Commun.* **2014**, *50*, 2635−7.
(23) *Bruker AXS TOPAS V4: General Profile and Structure Analysis Software for Powder Diffraction Data. User's Manual*; Bruker AXS: Karlsruhe, Germany. 2008.
(24) Renaudin, G.; Laquerriere, P.; Filinchuk, Y.; Jallot, E.; Nedelec, J. M. *J. Mater. Chem.* **2008**, *18*, 3593−600.
(25) Roh, H. S.; Hur, S.; Song, H. J.; Park, I. J.; Yim, D. K.; Kim, D. W.; Hong, K. S. *Mater. Lett.* **2012**, *70*, 37−9.
(26) Wu, C. C.; Chen, K. B.; Lee, C. S.; Chen, T. M.; Cheng, B. M. *Chem. Mater.* **2007**, *19*, 3278−85.
(27) Xia, Z. G.; Du, H. Y.; Sun, J. Y.; Chen, D. M.; Wang, X. F. *Mater. Chem. Phys.* **2007**, *119*, 7−10.
(28) Zhou, T. L.; Wang, H. R.; Liu, F. S.; Zhang, H.; Liu, Q. L. *J. Electrochem. Soc.* **2011**, *158*, H671−4.
(29) Zhang, Y. Y.; Xia, Z. G.; Wu, W. W. *J. Am. Ceram. Soc.* **2013**, *96*, 1043−6.
(30) Zhou, J.; Xia, Z. G.; Yang, M.; Shen, K. *J. Mater. Chem.* **2012**, *22*, 21935−41.
(31) Xia, Z. G.; Liu, R. S.; Huang, K. W.; Drozd, V. *J. Mater. Chem.* **2012**, *22*, 15183−9.